

# Combined Approach of Patch-Surfer and PL-PatchSurfer for Protein–Ligand Binding Prediction in CSAR 2013 and 2014

Xiaolei Zhu,<sup>†,‡</sup> Woong-Hee Shin,<sup>‡</sup> Hyungrae Kim,<sup>‡</sup> and Daisuke Kihara<sup>\*,‡,§</sup>

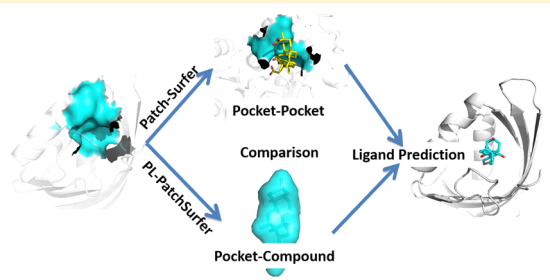
<sup>†</sup>School of Life Science, Anhui University, Hefei, Anhui 230601, China

<sup>‡</sup>Department of Biology Science, Purdue University, West Lafayette, Indiana 47907, United States

<sup>§</sup>Department of Computer Science, Purdue University, West Lafayette, Indiana 47907, United States

## Supporting Information

**ABSTRACT:** The Community Structure–Activity Resource (CSAR) benchmark exercise provides a unique opportunity for researchers to objectively evaluate the performance of protein–ligand docking methods. Patch-Surfer and PL-PatchSurfer, molecular surface-based methods for predicting binding ligands of proteins developed in our group, were tested on both CSAR 2013 and 2014 benchmark exercises in combination with an empirical scoring function-based method, AutoDock, while we only participated in CSAR 2013 using Patch-Surfer. The prediction results for Phase 1 task in CSAR 2013 showed that Patch-Surfer was able to rank all the four designed binding proteins within top ranks, outperforming AutoDock Vina. In Phase 2 of 2013, PL-PatchSurfer correctly selected the correct ligand pose for two target proteins. PL-PatchSurfer performed reasonably well in ranking ligands according to their binding affinity and in selecting near-native ligand poses in 2013 Phase 3 and 2014 Phase 1, respectively, although AutoDock Vina showed better performance. Lastly, in the 2014 Phase 2 exercise, the PL-PatchSurfer scores computed for ligands to target protein pairs correlated well with their  $\text{pIC}_{50}$  values, which was better or comparable to results by other participants. Overall, our methods showed fairly good performance in CSAR 2013 and 2014. Unique characteristics of the methods are discussed in comparison with AutoDock.



## 1. INTRODUCTION

Substantial progress has been made in the past two decades in developing virtual screening methods; however, developing accurate scoring functions for evaluating the binding energy of ligand–protein interactions is still a challenging problem.<sup>1,2</sup> A scoring function is aimed at not only identifying the correct docking pose of a ligand, but also differentiating the binding affinity between different small molecules.

Scoring functions can be classified into three different categories: molecular force fields,<sup>3–7</sup> statistical knowledge-based scoring functions,<sup>8–12</sup> and empirical scoring functions.<sup>13–16</sup> Force field scoring functions calculate potential energy between a protein and a small molecule, which usually contain several energy terms derived from the first-principles of physics, such as van der Waals, electrostatic, and hydrogen-bond interactions. Solvent effects are often included in an energy term as well. In contrast, statistical knowledge-based scoring functions are derived from the frequency of observed interacting atomic pairs and other structural features in a database of known protein–ligand complexes. Using the Boltzmann relationship, the observed frequency can be used to compute the energy of the structural feature.<sup>17</sup> Knowledge-based scoring functions do not provide individual energetic contributions to protein–ligand interactions, but they provide an efficient and practical way of calculating the binding affinity of ligands. Empirical scoring functions, the last category,

combine force field-based energy terms, knowledge-based terms, and other physically meaningful terms. Typically, weighting factors associated with different energy terms are calibrated by training on a set of known protein–ligand complexes with known binding affinity.

Since there are many different kinds of scoring functions, but none are sufficiently accurate while remaining efficient, it is important for the community to have objective benchmarks to validate and compare existing methods. In the past years, Dr. Heather Carlson and her team at the University of Michigan have been leading an effort to providing experimental data sets of crystal structures and binding affinities for diverse protein–ligand complexes, which are referred to as CSAR (Community Structure–Activity Resource, <http://www.csardock.org/>).<sup>18–21</sup> The 2013 CSAR benchmark exercise included selecting artificially designed proteins that bind to a ligand molecule, which made the exercise more interesting for the community. The 2014 CSAR exercise was to predict correct poses from sets of docking decoys and to rank-order compounds.

We participated and submitted predictions in CSAR 2013 using two methods of different types, Patch-Surfer<sup>22,23</sup> and

**Special Issue:** Community Structure Activity Resource (CSAR)

**Received:** October 13, 2015

AutoDock programs, AutoDock<sup>24</sup> and AutoDock Vina.<sup>25</sup> Patch-Surfer, which was developed in our group, makes binding ligand prediction for a target pocket by searching similar known ligand binding pockets. The method uses a local surface patch representation of binding pockets, which facilitates correct identification of local surface similarity and increases the search speed. In this article, we further extend our submitted predictions by applying our newly developed protein–ligand virtual screening method called PL-PatchSurfer,<sup>26–28</sup> which predicts binding ligands for a query binding pocket by directly evaluating complementarity between the protein pocket and ligands. PL-PatchSurfer was benchmarked in CSAR2013 Phase 2 and Phase 3, as well as CSAR2014 Phase 1 and 2.

Patch-Surfer performed very well in Phase 1 of CSAR 2013, being able to rank all four designed binding proteins that bind to a target ligand within top ranks. This performance was better than AutoDock Vina. In Phase 2 of 2013, PL-PatchSurfer correctly selected the correct ligand pose for two target proteins. PL-PatchSurfer performed reasonably well in ranking ligands according to their binding affinity in 2013 Phase 3 and in selecting a near-native ligand docking pose in 2014 Phase 1, although AutoDock Vina showed better performance. In the 2014 Phase 2 exercise, the PL-PatchSurfer scores computed for ligands to target protein pairs correlated well with their  $\text{pIC}_{50}$  values, which was better or comparable to results by other participants.

Although Patch-Surfer and PL-PatchSurfer employ rather coarse-grained molecular surface-based representations of binding pockets and ligands, which are very different from conventional virtual screening methods, they showed fairly good performance in CSAR 2013 and 2014. At the same time, comparison with performance of AutoDock and results with other participants revealed weaknesses of the methods. Unique strengths of Patch-Surfer and PL-PatchSurfer as well as weaknesses identified through the CSAR exercise are discussed.

## 2. METHODS

**2.1. Data Sets.** CSAR 2013 was based on the experimental data of artificially designed ligand-binding proteins by the David Baker's group at the University of Washington.<sup>29</sup> In the first phase, the organizers provided sequences of 16 designed proteins and a ligand molecule, a derivative of steroid digoxigenin. Its chemical structure in the SMILES representation is [C(C(=O)NCCC)O[C@H]1CC[C@]2([C@@H]-(C1)CC[C@H]1[C@@H]2C[C@H](O)[C@]2([C@]-1(O)CC[C@H]2[C@@H]1COC(=O)C1)C)C"]. The participants were asked to predict which proteins bind to the ligand and also to rank the binding ability of the designed proteins. In the second phase, the organizers provided the structures of two proteins and a set of pregenerated docking ligand decoys, and the participants were asked to score the provided poses and rank them. These two proteins were designed and produced by the Baker group from a putative isomerase (PDB ID: 1Z1S).<sup>29</sup> In the third phase, the organizers provided one protein structure, which is one of the two designed proteins whose crystal structures have been solved by the Baker group (PDB ID: 4J9A. This PDB ID was reported after the 2013 CSAR exercise) and 10 potential inhibitors. Participants were asked to predict the relative binding affinity of the 10 different inhibitors to the protein and predict the best three poses of each ligand.

Although we did not participate in CSAR 2014 at the time of the exercise, in this work, we tested PL-PatchSurfer on the

benchmark data sets provided in its two phases. For Phase 1, similar to Phase 2 of CSAR 2013, the organizers provided pregenerated 200 docking poses for 22 protein–ligand complexes. The target proteins were coagulation factor Xa (FXa) (three data sets each with a different ligand molecule), Spleen tyrosine kinase (SYK) (five sets), and tRNA-methyltransferase (TRMD) (14 sets). The participants were asked to find the nearest native pose to the crystal structure. Phase 2 of CSAR 2014 was a ligand ranking problem of given congeneric ligand sets for the three proteins in Phase 1. The five ligand sets were given to the participants, three for FXa, one for SYK, and one for TRMD, and each ligand set consisted of 31–276 ligands in the SMILES string format.

**2.2. Patch-Surfer.** Patch-Surfer is a program for predicting a binding ligand for a query protein by comparing the shape and physicochemical properties of a potential binding pocket of the query to known pockets in a database.<sup>22,23</sup> In Patch-Surfer, the pocket surface is represented by a set of overlapping local surface patches. A surface patch is characterized by four features: geometric shape, electrostatic potential, hydrophobicity, and visibility (concavity), each of which is described by three-dimensional Zernike descriptors (3DZD), which is a mathematical series expansion of a 3D function. Here, we briefly explain 3DZD. For more details, refer to the original papers.<sup>30,31</sup> To describe a surface with 3DZD, a surface patch is considered as a three-dimensional (3D) function,  $f(x)$ , in 3D space. To represent the geometric shape of a surface patch, the surface is mapped on a 3D grid, where 1s are placed for positions that are occupied by the surface and 0 otherwise. For the other properties, a 3D grid holds the property's value at each position. The 3D grid with mapped values is considered as a 3D function,  $f(x)$ . The function can be expanded into a series in terms of the Zernike–Canterakis basis:

$$\Omega_{nl}^m = \frac{3}{4\pi} \int_{|x| \leq 1} f(x) \overline{Z_{nl}^m(x)} dx \quad (1)$$

where

$$Z_{nl}^m(r, \theta, \phi) = R_{nl}(r) Y_l^m(\theta, \phi) \quad (2)$$

In this Zernike–Canterakis basis,  $R_{nl}(r)$  is the radial function and  $Y_l^m$  is the spherical harmonics.  $m$  and  $l$  are integers that have ranges  $-1 < m < 1$  and  $0 \leq l \leq n$ .  $\Omega_{nl}^m$  terms are called 3D Zernike moments, and the 3DZD,  $F_{nb}$ , are calculated as norms of vectors  $\Omega_{nl}$  as shown in eq 3. The norm gives rotational invariance to the descriptor.

$$F_{nl} = \sqrt{\sum_{m=-l}^{m=l} (\Omega_{nl}^m)^2} \quad (3)$$

To compare two pockets, similar patches from the two pockets are matched, and a similarity score is computed, which reflects the similarity of the features of matched patches and the relative positions of corresponding patches in each pocket.

Patch-Surfer was originally designed to compare the similarity between two protein pockets. In Phase 1 of the CSAR 2013 benchmark, we used Patch-Surfer in its original aim of comparing pockets. Two scoring terms, one for considering geometric shape similarity and another for comparing visibility (concavity), were used. In Phases 2 and 3, we modified the program so that it can compare the surface of a binding pocket with molecular surface of a small ligand molecule. For pocket-to-ligand comparison, we used scoring terms for shape and the

electrostatic potential to quantify complementarity of the two properties of a pocket and a ligand molecule.

**2.3. PL-PatchSurfer.** We ran PL-PatchSurfer for the benchmark data sets of Phase 2 and 3 of CSAR2013 and Phase 1 and 2 of CSAR2014. PL-PatchSurfer searches complementarity between a receptor pocket and a ligand by surface-patch comparison between the molecules represented by 3DZD. Thus, while Patch-Surfer compares a query pocket against known ligand binding pockets, PL-PatchSurfer compares a query pocket to ligands. Complementarity of a pocket and a ligand surface patch pair is evaluated in terms of shape, electrostatic potential, hydrogen-bond donor and acceptor positions, hydrophobicity, and the relative position of the patch in the molecule. In addition to the five features, the overall score of a pocket and a ligand considers similarity of the relative position of corresponding patches in each molecule. These terms were combined with weighting factors that were trained to maximize accuracy of virtual screening tests. To score given a ligand for a target pocket, a maximum of 50 3D structures of the ligand were generated from its SMILE representation using OMEGA.<sup>32</sup> Then, the surface of each conformation of the ligands was generated and converted into 3DZD. The score of a ligand for a target protein was defined as the maximum score among the scores computed for all the conformations of the ligand. For more details, refer to the original paper.<sup>26</sup>

**2.4. AutoDock Programs.** We used two versions of the AutoDock program, AutoDock4<sup>24</sup> and its subsequent version, AutoDock Vina.<sup>25</sup> Although both of the programs were developed by the same group, the scoring functions and sampling methods are different. AutoDock4 uses the Lamarckian Genetic algorithm and force field-based scoring function composed of van der Waals, Coulombic interaction, hydrogen bonding, solvation, and torsional entropy terms,<sup>24</sup> while AutoDock Vina uses Local Search and empirical scoring function with steric, hydrogen bonding, hydrophobic, and torsional entropy terms.<sup>25</sup> Weight parameters of both scoring functions that associate with these terms were calibrated using a set of protein–ligand complexes with known binding affinities. Although the same types of scoring terms were considered by the two programs, they have different implementations, and thus, performance can be different.<sup>25</sup> To run AutoDock4 and AutoDock Vina, input files of a target protein and a ligand were prepared with AutoDockTools (ADT) tools and Python scripts named `prepare_ligand4.py` and `prepare_receptor4.py`, which are associated with the AutoDock program. The binding pocket position in target protein was specified with the ADT molecular viewer. The parameters were kept at their default values.

For Phase 2 and Phase 3 in CSAR2013, we combined the scores from AutoDock Vina and Patch-Surfer, considering the complementary nature between the two. Because the scales of the two scores are different, we calculated the Z-score of each score and summed the two Z-scores as the final score.

### 3. RESULTS AND DISCUSSION

**3.1. Phase 1 Results.** The task of Phase 1 of the CSAR 2013 exercise was to identify proteins out of 16 artificially designed proteins that bind to a derivative of the steroid digoxigenin (SMILES of this molecule provided in the Data set section). Since only amino acid sequences of the 16 proteins were provided, we needed to model 3D structures of the proteins. The modeling was performed using threading web servers, HHpred<sup>32</sup> and LOMETS,<sup>33</sup> both of which build a

structure model of a query protein based on a known protein structure that is used as a template. LOMETS takes a meta-server approach, which runs 10 independent prediction programs. Thus, by adding HHpred, we had 11 independent predictions for each target protein. Among the 11 structure models, we have selected the one which was built based on a template protein selected by the majority of the programs. The left columns of Table 1 shows the templates identified by this

**Table 1. Template Proteins Used for Building Target Proteins in 2013 Phase 1 Exercise**

target ID	PDB ID <sup>a</sup>	high sequence identity template <sup>a</sup>	low sequence identity template <sup>b</sup>	
		sequence identity (%)	PDB ID	sequence identity (%)
DIG1	1GY7B	86.9	1ZO2A	39.3
DIG2	1MVEA	89.9	1CPNA	27.5
DIG3	1YNAA	81.3	3AKQA	54.7
DIG4	3JUMB	87.9	3FF0A	48.3
DIG5	1Z1SA	91.5	1S5AA	36.1
DIG6	3CU3A	80.0	4I4KA	25.2
DIG7	3GWRB	86.2	3CNXA	24.2
DIG8	3HK4A	78.1	5AIGA	23.9
DIG9	1I60A	88.2	2ZVRA	22.1
DIG10	1Z1SA	92.2	1S5AA	35.3
DIG12	2OWPA	88.8	2RCDA	46.5
DIG13	2OX1A	90.8	4CNNA	19.6
DIG14	3E5ZA	92.0	3DR2A	28.3
DIG17	3CU3A	85.0	4I4KA	24.6
DIG18	1Z1SA	89.9	1S5AA	35.3
DIG19	1Z1SA	86.0	1S5AA	33.6

<sup>a</sup>Templates with a high sequence identity to the target proteins.

<sup>b</sup>Templates with a low sequence identity to the targets. The models were used in the post-analyses to investigate how the quality of homology models affects the predicting ligand-binding proteins.

procedure for building the target proteins and the sequence identity between each template to its target protein. The structure models were expected to be sufficiently accurate for the subsequent docking prediction because the sequence identities were all very high. Indeed, RMSD of C $\alpha$  atoms of the model structure for DIG19 to its crystal structure that was revealed after the Phase 1 experiment (PDB ID: 4J9A) was 0.602 Å (Figure 1).

For further post-analysis, we have also constructed a model for each target protein using a template structure that has a lower sequence identity to the target (right columns in Table 1). Later in this section we investigate how the model quality affects the accuracy of selecting targets that bind to the ligand.

We applied Patch-Surfer to the homology models to determine which proteins have a binding pocket that is the most similar to known steroid binding pockets. The reference steroid binding pockets were identified by keyword searches on the PDB web site. Two entries of steroid binding proteins were found, 1HDC (20 $\beta$ -hydroxysteroid dehydrogenase) and 3UP0 (nuclear receptor DAF-12). 1HDC has bound carbenoxolone (PDB ID: CBO) in the crystal structure, while 3UP0 has bound (5 $\beta$ , 14 $\beta$ , 17 $\alpha$ , 25S)-3-oxocholest-7-en-26-oic acid (PDB ID: D7S). Among these two PDB entries, we decided to use 1HDC as the reference because its ligand, CBO, has five ring structures, which is consistent with the target ligand.

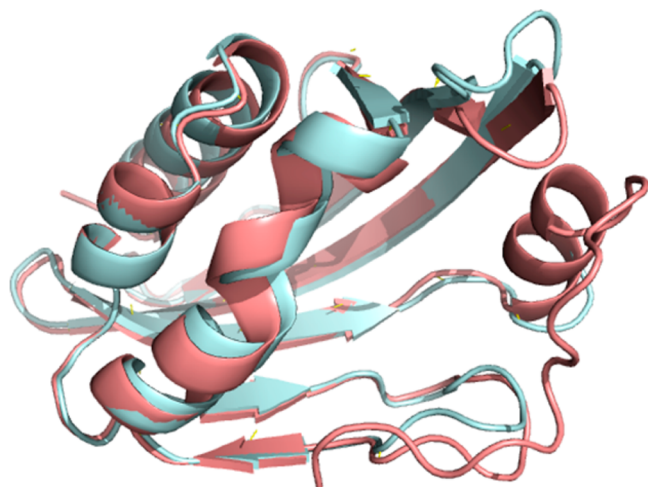


**Figure 1.** Superposition between the model and the crystal structure of DIG19 (PDB ID: 4J9A). The crystal structure is showed in cyan, and the modeled structure is shown in pink. The RMSD between the model and the crystal structure is 0.602 Å.

**Table 2** shows the rank of the 16 proteins based on the Patch-Surfer score, which quantifies the similarity of the

**Table 2. Rank of Predicted Binding Affinity of Target Designed Proteins Using Patch-Surfer<sup>a</sup>**

rank	target protein	Patch-Surfer score <sup>b</sup>	binding or not
1	DIG5	0.592	yes (205 μM)
2	DIG8	0.653	no
3	DIG19	0.684	yes (541 pM)
4	DIG10	0.686	yes (8.9 μM)
5	DIG18	0.688	yes <sup>c</sup>
6	DIG9	0.702	no
7	DIG2	0.711	no
8	DIG3	0.723	no
9	DIG13	0.724	no
10	DIG6	0.729	no
11	DIG7	0.752	no
12	DIG4	0.785	no
13	DIG12	0.789	no
14	DIG17	0.802	no
15	DIG14	0.847	no
16	DIG1	0.963	no

<sup>a</sup>Eight targets in bold (DIG5 to DIG3 in the table) were predicted to bind the target ligand. <sup>b</sup>Small Patch-Surfer score indicates that the putative binding pocket is similar to the reference steroid binding pocket. <sup>c</sup>Binding affinity of this protein is not available because it was not reported in the paper by Tinberg et al.<sup>29</sup>

pockets in the targets and the steroid binding pocket of 1HDC. Since the Patch-Surfer score is meaningful in ranking proteins relative to each other but does not provide an absolute indication of ligand binding, we decided to submit the eight top-ranked target proteins as binders. They are, DIG5, DIG8, DIG19, DIG10, DIG18, DIG9, DIG2, and DIG3. The Patch-Surfer's prediction was very successful in ranking all three positive proteins, whose binding affinity to DOG was confirmed by experiments to be in the  $\mu\text{M}$  range, within the top four ranks. Shown in **Figure 2** are the crystal structures of 1HDC and the designed protein (DIG19) with bound ligands, which show that the ligands have similar binding mode in the

two pockets. In both proteins, the ligands bind vertically in the pockets and the hydrophobic ring structures in the ligands (picene ring and phenanthren ring for the ligands of 1HDC and DIG19, respectively) bind to a hydrophobic core of the pockets.

For Phase 1 of CSAR 2013 exercise, there were 16 predictions submitted. Among them, only four of them, including Patch-Surfer, correctly ranked all four binding proteins within top five ranks. Thus, Patch-Surfer was successful relative to the other participants in the benchmark exercise.

Besides the prediction by Patch-Surfer (**Table 2**), we also submitted a separate prediction in parallel that used a combined score of Patch-Surfer and four modes of AutoDock. Three scores are computed from AutoDock: one by flexible docking by AutoDock Vina, which explores various conformations of a ligand that give the lowest energy; another score by the Vina rigid docking mode, which treats a ligand as a rigid molecule; and last, a score by the AutoDock4 flexible docking mode. With Patch-Surfer, we computed two scores, the pocket similarity score for the binding pocket of each target and either of 1HDC or 3UP0. Thus, in total, we had five different scores. These five scores were then normalized by computing a Z-score, and the sum of the five Z-scores was used to obtain the final rank of the target proteins (**Table 3**). It turned out that this prediction was worse than the Patch-Surfer's prediction in **Table 2**, not being able to select the best binder, DIG19, within top half of the targets.

After CSAR2013, we extended the analysis in two directions to further understand the performance of Patch-Surfer. First, we made homology models of the designed proteins using templates with a lower sequence identity and examined how prediction results are affected by the quality of the models. Second, we used a variety of ligand binding pockets as the reference to investigate how they influence prediction results.

The right columns in **Table 1** show template structures with a lower sequence identity used to build homology models for the first part of the extended analysis. These templates were identified by HHpred, and the models were generated using MODELER<sup>34</sup> based on the templates. The structural difference of the models with close and distant templates is not large; on average, RMSD between them was 2.17 Å (**Table 4**, rightmost column). The RMSD is even smaller, 0.98 Å, for the models of ligand binding proteins, DIG5, DIG10, DIG18, and DIG19. However, this difference in models made a substantial difference in the prediction results (**Table 4**). Among the four ligand binding proteins, only DIG5 was ranked within the top, while the other three proteins were below the half of the rank. By performing docking of the target ligand, the derivative of digoxigenin, to the structure models, it turned out that this difference was enough to make very different binding modes of the ligand to the proteins (**Figure 3**). The models built with high sequence identity templates (**Figure 3A, C, E, G**) have one larger pocket that is consistent with the reference steroid binding protein, 1HDC. On the other hand, the corresponding pockets in the models built on lower sequence identity templates are smaller, which caused the positions of bound ligands on the other side of the helix in the middle of the structures. These results suggest that, when computational protein models are used in ligand-binding prediction, their quality is critical to prediction results.

For the second post-analysis, we examined how different reference pockets affect the Patch-Surfer results. In addition to

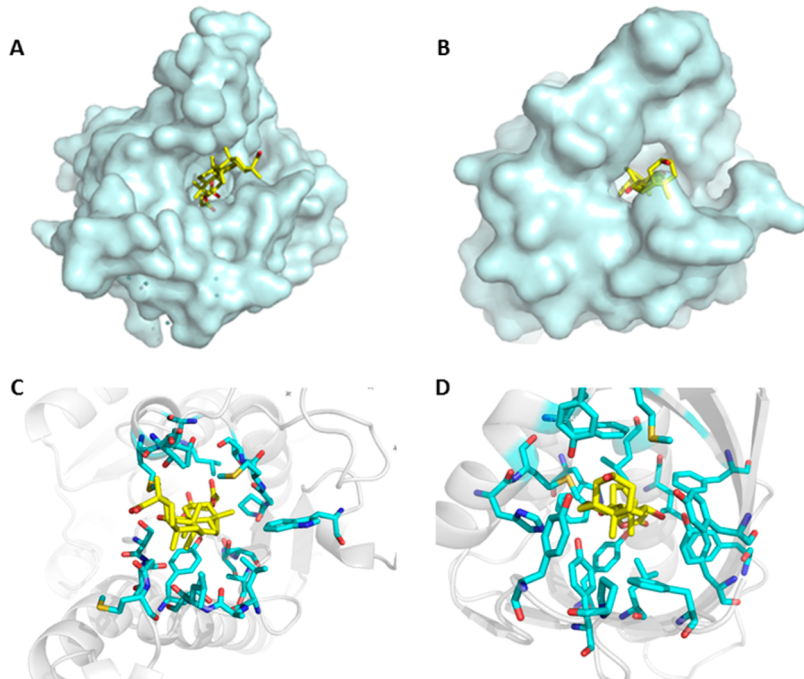


**Figure 2.** Crystal structures of 1HDC and the designed protein DIG19 (PDB ID: 4J9A). Ligands are shown in yellow. The ligands of 1HDC and DIG19 are carbenoxolone and digoxigenin, respectively. (A, B) Overall structure of 1HDC and DIG19, respectively. (C, D) Binding sites of 1HDC and DIG19, respectively.

**Table 3. Rank of Predicted Binding Affinity of Designed Proteins Using the Combined Score<sup>a</sup>**

rank	target protein	total Z-score	binding or not
1	DIG5	-4.21	yes (205 uM)
2	DIG18	-2.71	yes
3	DIG10	-2.61	yes (8.9 uM)
4	DIG2	-2.30	no
5	DIG3	-2.21	no
6	DIG8	-1.95	no
7	DIG4	-1.47	no
8	DIG17	-1.27	no
9	DIG6	-0.83	no
10	DIG13	-0.65	no
11	DIG14	-0.59	no
12	DIG19	0.48	yes (541 pM)
13	DIG9	2.03	no
14	DIG7	2.51	no
15	DIG12	2.93	no
16	DIG1	12.87	no

<sup>a</sup>Target proteins in bold (top eight targets) were predicted to bind to the target ligand.

1HDC we originally used as the reference pocket, we newly selected nine more protein–ligand complexes as the references. These additional compounds were identified by the SIMCOMP web server<sup>35</sup> using the target ligand as the query molecule. Using Patch-Surfer, a reference pocket was compared with binding pockets of the structure models of the 16 target proteins built based on the high sequence identity templates, and the target proteins were ranked according to the Patch-Surfer pocket similarity scores. The nine binding pockets and their bound ligands are listed in Table 5 with five distance (i.e., dissimilarity) scores to the target ligand. Their two-dimensional (2D) structures are shown in Figure 4. All of the compounds

**Table 4. Rank of Predicted Binding Affinity of Target Designed Proteins Using Structure Models with a Lower Quality**

rank	target protein	Patch-Surfer score	binding or not	RMSD (Å) <sup>a</sup>
1	DIG5	0.592	yes (205 uM)	1.02
2	DIG13	0.614	no	3.31
3	DIG14	0.626	no	0.86
4	DIG9	0.645	no	2.80
5	DIG6	0.657	no	4.83
6	DIG4	0.675	no	0.36
7	DIG7	0.680	no	1.86
8	DIG8	0.688	no	3.35
9	DIG18	0.689	yes	0.93
10	DIG2	0.696	no	3.83
11	DIG3	0.734	no	0.60
12	DIG10	0.742	yes (8.9 uM)	1.00
13	DIG12	0.742	no	0.48
14	DIG17	0.767	no	7.67
15	DIG19	0.768	yes (541 pM)	0.97
16	DIG1	0.988	no	0.91

<sup>a</sup>RMSD between the model constructed using a low sequence identity template (right column in Table 1) and the model using a high sequence identity template (left columns in Table 1).

but CBO share the four ring structure, cyclopenta[a]-phenanthrene, with the target ligand (bottom right corner in Figure 4). The five compound distances measure different aspects of compounds, and thus, their distances are not necessarily consistent. Zernike (3D Zernike descriptors) compares global surface shape of molecules.<sup>28,31,36</sup> SIMCOMP evaluates 2D graph similarity of molecules.<sup>35</sup> LIGSIFT compares molecules by overlapping Gaussian distributions that represent the global shape of the molecules. We used two options of LIGSIFT, one that considers the shape only (LIGSIFT\_SHP) and the other that also considers the

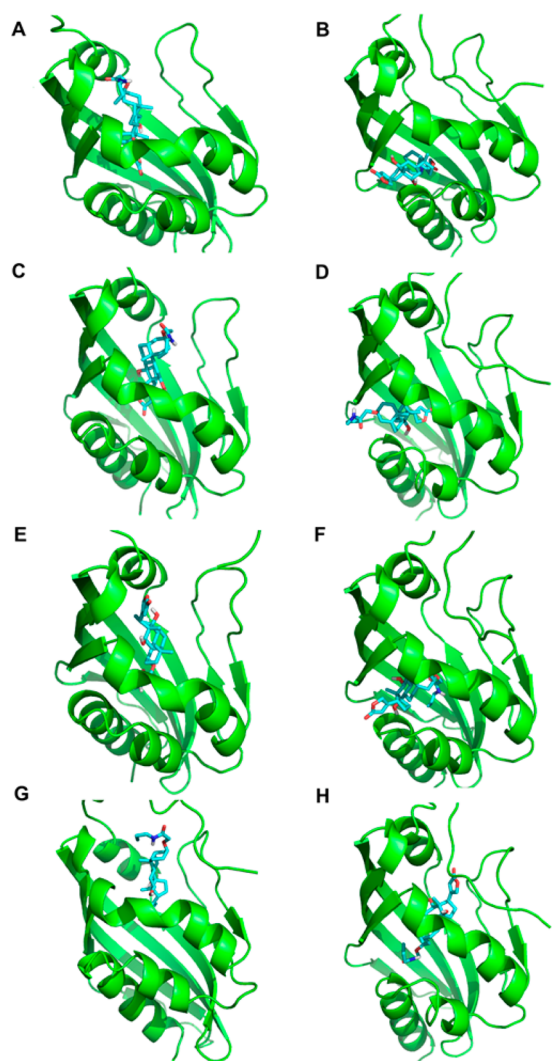


**Figure 3.** Predicted binding mode using models built on high and low sequence identity templates. At each row, the structure on the left/right is a model based on the high/low sequence identity template. The target ligand was docked using the AutoDock Vina in the flexible docking mode. The lowest energy structures are shown: (A, B) DIG5, (C, D) DIG10, (E, F) DIG18, and (G, H) DIG19.

chemical nature of molecules (LIGSIFT\_CHEM).<sup>37</sup> The last one is the Tanimoto coefficient computed with the Open Babel software,<sup>38</sup> which indicates the fraction of common fingerprints of molecules.

On the right side of **Table 5**, Patch-Surfer's predictive accuracies computed using each of the 10 reference binding pockets are shown. The accuracies are represented in terms of the Area Under the Receiver Operator Characteristics Curve (AUC), Top 4, Top 6, and Top 8 accuracies. Top 4, 6, and 8 accuracies show the ratio of the four designed proteins that bind the target ligand (DIG5, DIG10, DIG18, and DIG19) ranked within each respective rank. Using 1HDC as the reference pocket performed best, with an AUC value and Top 4, 6, and 8 accuracies of 0.938, 0.75, 1.00, and 1.00, respectively. The second and the third well-performed pockets were 3AQI and 3A3Y. Interestingly, the bound ligands of these three proteins, 1HDC, 3AQI, and 3A3Y, are not particularly similar to the target ligand, according to the five compound distance measures. In **Table 6**, we further computed Pearson's correlation coefficient between compound distance measures and accuracy measures. Global shape difference measured with 3D Zernike descriptors (3DZD) and SIMCOMP showed a relatively large correlation to the accuracy measures, but overall, the correlations were not substantially high between those ligand distance measures and the predictive accuracies. The reason for the highest correlation to the accuracies with the Zernike distance might be because Patch-Surfer uses the 3DZD for describing binding pocket surface properties, although the way 3DZD is used for the ligand distance measure and for Patch-Surfer is different. The former uses it for representing global shape of ligands, while the latter uses it for representing segmented pocket surface regions.

The two post-analyses revealed that the original choices of the templates and the reference pocket we made were very appropriate. The analyses also confirm that the qualities of homology models are very important in ligand binding prediction as also reported by previous works.<sup>39–41</sup>

**3.2. 2013 Phase 2 Results.** In Phase 2 of the CSAR 2013 exercise, the organizers provided structures of two proteins, DIG18 and DIG20 (PDB ID: 4J8T), as well as 200 pregenerated ligand poses of the target ligand, for both of the proteins. Participants were asked to score those 200 ligand

**Table 5. Distance (dissimilarity) of Bound Ligands of 10 Different Reference Pockets and Predictive Accuracy Using References in Post-Analysis for 2013 Phase 1**

PDB code	ligand	distance of ligand to target ligand <sup>a</sup>					prediction results <sup>b</sup>			
		Zernike	SIMCOMP	LS_SHP	LS_CHEM	Babel	AUC	Top 4 Acc	Top 6 Acc	Top 8 Acc
1hdc	CBO	0.698	0.727	0.0122	0.0246	0.587	0.938	0.75	1.00	1.00
1lke	DOG	0.546	0.375	0.0075	0.0133	0.287	0.417	0.25	0.25	0.25
2b04	CHO	0.678	0.459	0.0405	0.0725	0.578	0.646	0.25	0.50	0.75
3a3y	OBN	0.739	0.440	0.0131	0.0254	0.431	0.688	0.50	0.75	0.75
3aqi	CHD	0.578	0.460	0.0160	0.0286	0.687	0.875	0.75	0.75	0.75
4res	BUF	0.590	0.277	0.0117	0.0203	0.863	0.312	0.25	0.25	0.25
4jch	1KG	0.568	0.650	0.0220	0.0409	0.571	0.646	0.25	0.50	0.75
2q1v	PDN	0.624	0.589	0.0197	0.0341	0.660	0.438	0.25	0.50	0.50
1q23	FUA	0.697	0.724	0.0444	0.0884	0.553	0.604	0.50	0.50	0.50
3b0w	DGX	0.519	0.517	0.0198	0.0485	0.441	0.542	0.25	0.50	0.50

<sup>a</sup>Distance (dissimilarity) of the bound ligand in each PDB entry to the actual compound, the derivative of digoxigenin, was computed using five compound comparison methods. For the SIMCOMP score and the Tanimoto Coefficient computed with Babel, the original value was subtracted from 1.0 to make all the distance values consistently smaller for more similar ligands. <sup>b</sup>AUC, Area Under the Receiver Operator Characteristic Curve. Top 4, 6, and 8 accuracies compute the fraction of the four binding proteins (DIG5, DIG10, DIG18, DIG19) within top ranks.

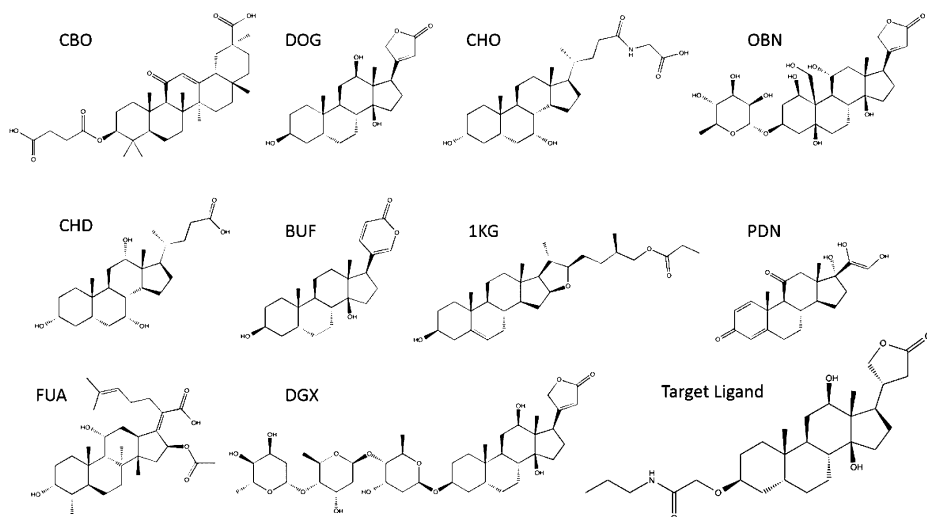


**Figure 4.** Bound ligands of the 10 reference pockets used in Table 5.

**Table 6. Pearson's Correlation Coefficients between Reference Ligand Dissimilarity to Target Ligand and Predictive Accuracies of Patch-Surfer in CSAR 2013 Phase 1**

	AUC	Top 4 Acc	Top 6 Acc	Top 8 Acc
Zernike	0.400	0.433	0.532	0.504
SIMCOMP	0.516	0.360	0.534	0.559
LIGSIFT_SHP	0.067	-0.110	-0.070	0.131
LIGSIFT_CHEM	0.075	-0.097	-0.049	0.117
Babel	-0.047	0.115	0.008	0.020

poses to identify the correct pose of the ligand. We submitted two predictions for this phase, one by using AutoDock Vina in the score only mode and the other one by using the consensus score between Vina and Patch-Surfer. Moreover, we ran PL-PatchSurfer for this exercise as a post-analysis.

All the three methods successfully selected the correct pose of the ligand with the lowest score among all the pregenerated poses. Figure 5 shows the distribution of the scores and the RMSD of the 200 ligand poses of DIG18 (Figure 5A, B, C) and DIG20 (Figure 5D, E, F). Spearman's rank coefficients between the Vina results and the consensus results were 0.642 and 0.886 for DIG18 and DIG20, respectively, which indicate that the ranks by the two scores are different but correlated. To run PL-PatchSurfer, we used the binding pocket of an engineered lipocalin protein structure (PDB ID: 1LKE), which was co-crystallized with digoxigenin (DOG), instead of using the homology models prepared for Phase 1. Ligand poses that have an RMSD of 10 Å or higher to the reference binding pose of 1LKE were not scored because they were obviously dissimilar to the reference pose.

**3.3. 2013 Phase 3 Results.** In Phase 3 of the CSAR 2013 exercise, the organizer provided the 3D structure of one of the artificially designed proteins, DIG19 (PDB ID: 4J9A), and 10 different small molecules. Participants were asked to find the correct binding pose of each ligand and its corresponding binding affinity. We used Vina to generate a set of ligand poses and used the Vina score and the consensus of Vina and Patch-Surfer scores to rank the poses. AutoDock Vina was run in the flexible docking mode. For the most cases, Vina generated nine poses (Table S1, Supporting Information). In addition to the submitted predictions, we newly ran PL-PatchSurfer as a post-analysis of this exercise.

Figure 6A shows how the Vina score predicted the rank of the ligands in the order of their binding affinity. The ligands were ranked in two ways. First, we ranked them based on the Vina score of the lowest energy conformation among those which were generated (circles, Figure 6A). Next, we ranked the ligand using the average of the top three lowest energies among the generated conformations (triangles). Overall, predicted ranks showed reasonable agreement with the experimental results. The two highest affinity ligands (left bottom corner) were ranked correctly when the average score of the three best poses was considered and also were selected by the best pose energy as the two best binders but with reversed rank. Moreover, the ligand with the lowest affinity (right upper corner) was selected correctly when considering the best pose energy. The correlation coefficient between the best Vina score (filled circles) and the experimental  $pK_d$  was 0.819, while it was 0.834 when the average score of the three best poses was considered (empty circles) (Figure 7A).

Next, in Figures 6B and 7B, we examined how the combined score of Vina and Patch-Surfer works for ranking and predicting binding affinity of ligands. The results were not as good as using the Vina score only (Figures 6A and 7A). The correlation coefficients were -0.344 and -0.394, when the best score (filled circles) and the average of the three best scores (empty circles) were used, respectively.

At last, PL-PatchSurfer's results on this benchmark are shown in Figure 8. Pearson's correlation coefficient between the PL-PatchSurfer score and  $pK_d$  phase is -0.41. Although this is not a strong correlation, it shows that the program could discriminate nonbinders from active compounds, as it is originally designed. The PL-PatchSurfer's correlation is not as good as that of AutoDock Vina but better than the combined score of Vina and Patch-Surfer.

According to the CSAR organizer's paper,<sup>42</sup> our results using Vina is the sixth among 27 predictions submitted to this phase, a larger correlation (0.819 and 0.834), while the results with the combined score and PL-PatchSurfer were among the lower ranks.

**3.4. Results for Phase 1 of CSAR 2014.** We did not submit our predictions for CSAR 2014, but here, we report results of PL-PatchSurfer that we newly ran on the exercise data sets of Phase 1 and 2. The data set of Phase 1 contained 22 protein-ligand pairs with 200 pregenerated decoys for each

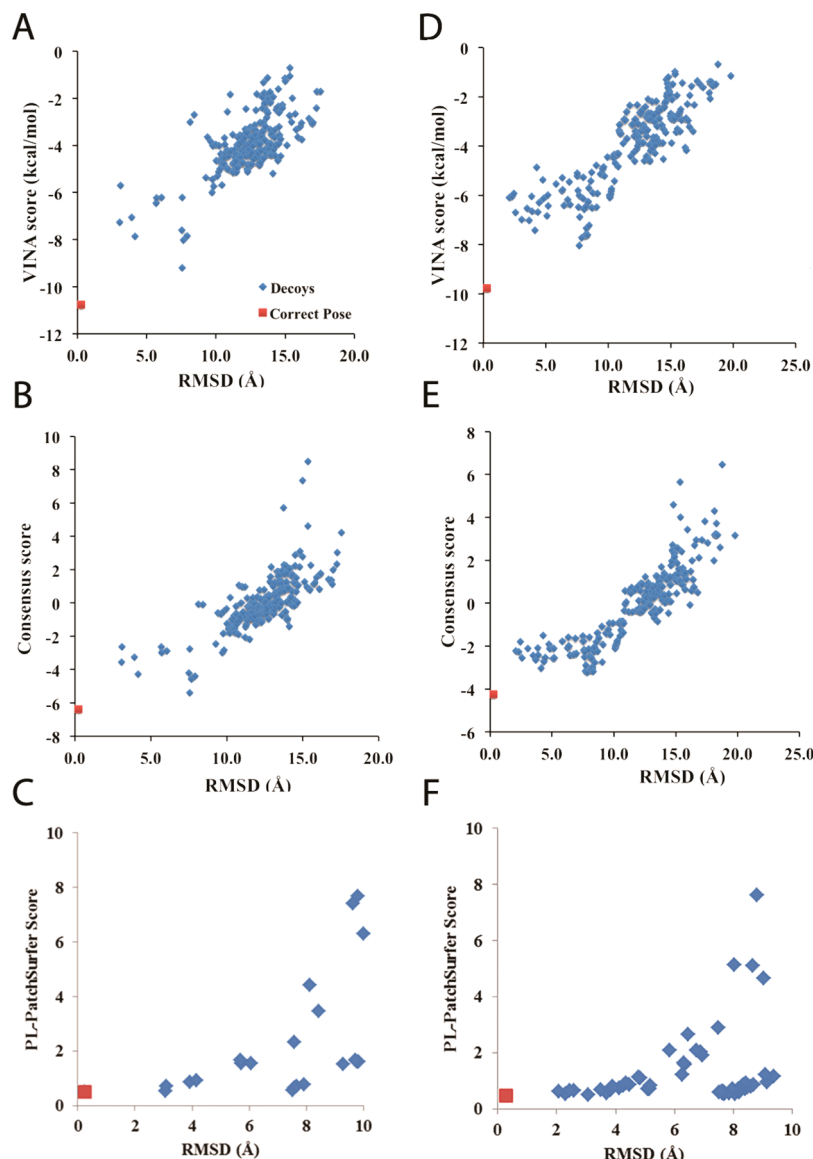


**Figure 5.** Score distributions relative to the RMSD of ligand poses. The correct pose is shown in red and the other poses are in blue. Panels A, B, C are for DIG18, and panels D, E, F are results for DIG20. A and D show results using the Vina score, B and E used the consensus score, and C and F used PL-PatchSurfer. In C and F, the ligand poses that have an RMSD of 10 Å or higher to the reference binding pose of 1LKE were not scored because they were obviously dissimilar to the reference.

ligand. The target proteins were FXa, SYK, and TRMD. Participants were asked to score the decoy poses for each protein–ligand pair. To apply PL-PatchSurfer in this phase, weighting factors of the PL-PatchSurfer scoring function were trained for each of the three target proteins using five crystal structures each for the target proteins (FXa: 2PR3, 2VVV, 2VWO, 2WYG, and 3CEN; SYK: 1XBB, 3TUC, 4FYO, 4PV0, and 4PX6; TRMD: 1P9P, 4MCB, 4MCC, 4MCD, and 4YVJ). The ligands of these crystal structures were not the same as the target ligands of this exercise. Using the crystal structures, decoy conformations of the cognate ligand for each target protein were generated by DOCK6.<sup>43</sup> The average number of the generated decoys were 763.4, 701.2, and 259.0 for FXa, SYK, and TRMD, respectively. Using the decoys, the weights were trained to maximize the Pearson’s correlation coefficients between RMSD of the docked ligand and the PL-PatchSurfer score of the decoys.

**Table 7** summarizes the results of PL-PatchSurfer’s prediction. PL-PatchSurfer was able to select the nearest native (i.e., correct) pose as the top 1 choice for two out of three FXa decoy sets and three out of five SYK decoy sets. As for the TRMD decoy sets, although the top 1 rank was correct only for one out of 14 set sets, the top 1 rank was within 2 Å RMSD from the nearest-native binding pose for additional nine cases. When top 3 ranks were considered, the correct pose was selected for the all three FXa decoy sets, four out of five SYK sets, and five TMSD sets. If the consideration was further extended to top 10 ranks, correct poses were selected for all but three decoy sets. Although these results by PL-PatchSurfer are not as high as AutoDock Vina that we have also applied (Table S2, *Supporting Information*), it shows that PL-PatchSurfer is able to predict a near native pose within a top rank.

**3.5. 2014 Phase 2 Results.** The exercise for Phase 2 of CSAR2014 was to rank the ligands in the given ligand library in terms of their pIC<sub>50</sub> values (three sets for FXa, one set for SYK,

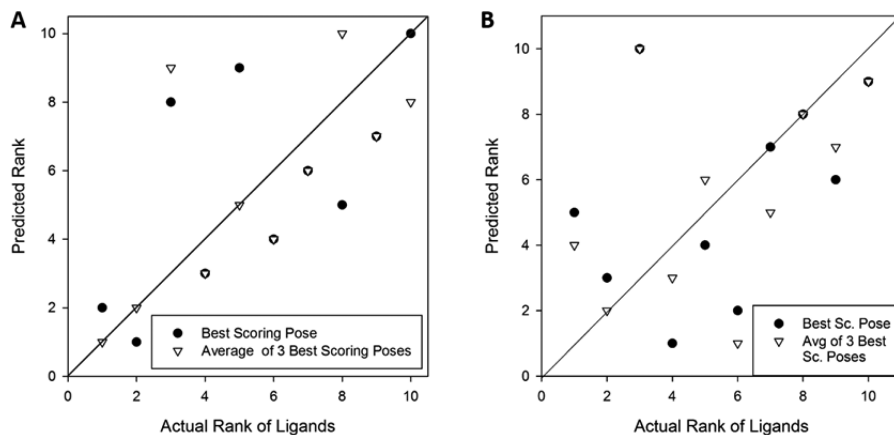


**Figure 6.** Correct and predicted rank of the 10 ligands in CSAR 2013 Phase 3. (A) Ranks of ligands were predicted by AutoDock Vina scores. (B) Prediction of the rank was performed by the combined scores of Vina and Patch-Surfer. Filled circles: ranking of the ligands based on the lowest energy (score) among the constructed conformations for the ligands. Triangles: ranking based on the average of the lowest three energies (scores) among the constructed conformations for the ligands.

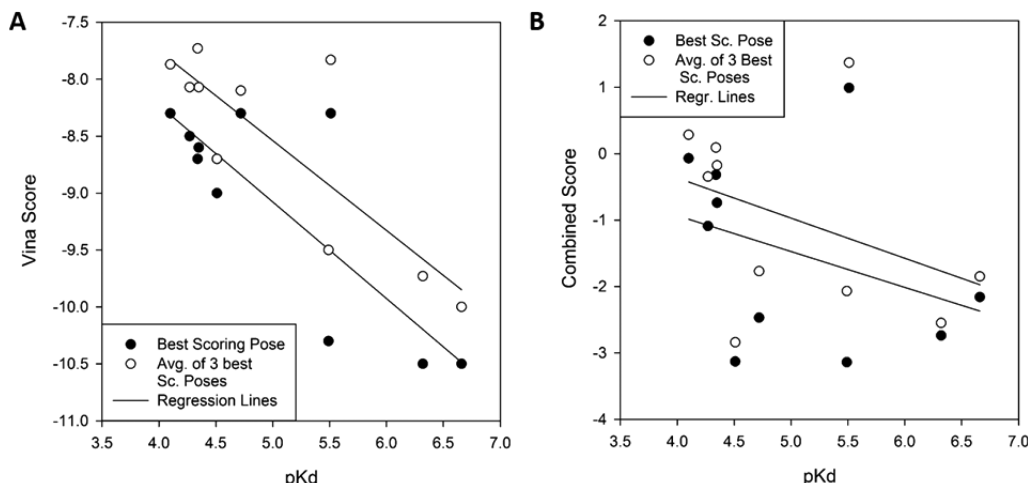


**Figure 7.** Correlation between the scores and experimentally determined  $pK_d$  in 2013 Phase 3. Filled circles are the lowest energy (score) among the constructed conformations and are plotted for each ligand. Empty circles are the average of the three lowest energies (scores) among the constructed conformations and are plotted for each ligand. Lines are linear regression between  $pK_d$  and the scores. (A) Correlation with the Vina score of the ligands. (B) Correlation with the combined score of Vina and Patch-Surfer.

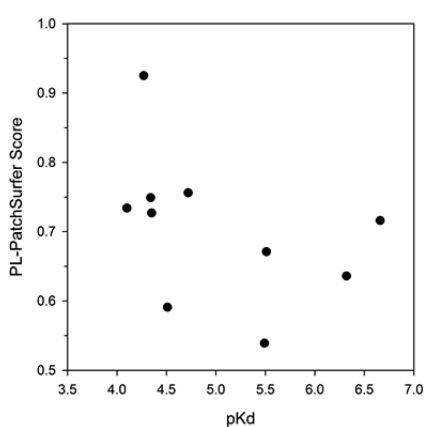


**Figure 8.** Correlation between the PL-PatchSurfer score and  $pK_d$  in 2013 Phase 3.

and one set for TRMD). The numbers of ligands in the library are 45, 67, and 51 for the three sets for FXa, 31 for TRMD, and 276 for SYK. We used PL-PatchSurfer to compute the scores

for all the ligands and compared the scores with provided  $pIC_{50}$  values by computing the Pearson's correlation coefficients (Table 8). Moderate correlation coefficients of  $-0.590$  and  $-0.671$  were observed for the data set 1 of FXa and TRMD, respectively. Correlation was weak for the other cases. However, when compared with results of other participants<sup>44–46</sup> that were available at the time of writing (Table 8), PL-PatchSurfer was the best among the other available prediction results for FXa data set 1 and competitive for TRMD.

#### 4. CONCLUSIONS AND DISCUSSION

The CSAR benchmark exercise provided a unique opportunity for researchers who develop or use protein–ligand docking methods to objectively evaluate the performance of such methods. We participated in all three phases of CSAR 2013 and submitted our predictions. In the submitted predictions, we used Patch-Surfer in combination with AutoDock. Moreover, in this work, we have further used PL-PatchSurfer to complete exercises provided in CSAR 2014. Patch-Surfer and PL-PatchSurfer are both for predicting binding ligands for a

**Table 7. PL-PatchSurfer's Results of CSAR 2014 Phase 1**

Target	Top 1 <sup>a</sup>	Top 3	Top 5	Top 10
01_FXA_gtc101	X <sup>b</sup>	X	X	X
02_FXA_gtc398	1.630	X	X	X
03_FXA_gtc401	X	X	X	X
04_SYK_gtc224	2.053	1.550	1.550	1.550
05_SYK_gtc225	X	X	X	X
06_SYK_gtc233	2.370	X	X	X
07_SYK_gtc249	X	X	X	X
08_SYK_gtc250	X	X	X	X
09_TRMD_gtc445	3.214	3.096	X	X
10_TRMD_gtc446	3.181	3.095	X	X
11_TRMD_gtc447	1.772	1.772	1.772	X
12_TRMD_gtc448	2.564	2.564	2.541	X
13_TRMD_gtc451	1.614	X	X	X
14_TRMD_gtc452	1.746	1.477	1.477	1.477
15_TRMD_gtc453	1.501	1.501	X	X
16_TRMD_gtc456	3.920	X	X	X
17_TRMD_gtc457	1.536	X	X	X
18_TRMD_gtc458	1.602	1.602	X	X
19_TRMD_gtc459	1.721	1.710	1.495	X
20_TRMD_gtc460	1.442	X	X	X
21_TRMD_gtc464	X	X	X	X
22_TRMD_gtc465	1.919	1.919	1.919	1.919

<sup>a</sup>Lowest RMSD ( $\text{\AA}$ ) within top 1, 3, 5, and 10 were reported. <sup>b</sup>X shows that the best pose (pose that is nearest to the native) was selected within the specified top hits. The values are RMSD from the best pose ( $\text{\AA}$ ).

query pocket in a protein surface, but they achieve this in complementary ways; the former is designed to compare a query pocket against a database of known ligand binding pockets, while the latter compares molecular surface of ligands to a query pocket.

It was a pleasant surprise that Patch-Surfer performed well in 2013 Phase 1, even better than AutoDock, in selecting designed proteins that bind to the target ligand. PL-PatchSurfer performed well in 2013 Phase 2 in identifying correct binding pose of ligands and in 2014 Phase 2 in terms of correlation to  $\text{pIC}_{50}$ . In 2014 Phase 2, PL-PatchSurfer performed the best among other available participants' results in one of the data sets (FXa data set 1) and also better or comparable in another set (TRMD). On the other hand, PL-PatchSurfer showed weakness in 2013 Phase 3 and 2014 Phase 1, whose aims were ranking of ligands and ligand binding poses, respectively, which probably needed more detailed atomic energy evaluation than PL-PatchSurfer is equipped with. The surface-based coarse-

grained molecular representation used in PL-PatchSurfer seemed to not work well in these two exercises; however, the coarse-grained representation can be an advantage in certain situations, including virtual screening for binding pockets in apo form as we showed in our recent study.<sup>27</sup> Thus, it is important to use the methods for appropriate purposes for their algorithms and to know their characteristics and when they show their strengths.

## ■ ASSOCIATED CONTENT

### S Supporting Information

The Supporting Information is available free of charge on the ACS Publications website at DOI: 10.1021/acs.jcim.5b00625.

Number of poses for each ligand generated by Autodock Vina in Phase 3 CSAR 2013 exercise, Autodock Vina scores for protein–ligand pairs of CSAR 2014 Phase 1 using two different atom charge assignments, and Vina score distributions with the two different atom charges on the 22 target–ligand data set in Phase 1 of CSAR 2014. (PDF)

## ■ AUTHOR INFORMATION

### Corresponding Author

\*E-mail: dkihara@purdue.edu. Phone: +1-765-496-2284.

### Notes

The authors declare no competing financial interest.

## ■ ACKNOWLEDGMENTS

The authors thank Lenna Peterson for proofreading the manuscript. This work was partly supported by the National Institute of General Medical Sciences of the National Institutes of Health (R01GM097528), the National Science Foundation (IIS1319551, DBI1262189, IOS1127027), and the National Natural Science Foundation of China (21403002).

## ■ REFERENCES

- Warren, G. L.; Andrews, C. W.; Capelli, A. M.; Clarke, B.; LaLonde, J.; Lambert, M. H.; Lindvall, M.; Nevins, N.; Semus, S. F.; Senger, S.; Tedesco, G.; Wall, I. D.; Woolven, J. M.; Peishoff, C. E.; Head, M. S. A critical assessment of docking programs and scoring functions. *J. Med. Chem.* **2006**, *49* (20), 5912–5931.
- Cheng, T.; Li, X.; Li, Y.; Liu, Z.; Wang, R. Comparative assessment of scoring functions on a diverse test set. *J. Chem. Inf. Model.* **2009**, *49* (4), 1079–1093.
- Ewing, T. J.; Makino, S.; Skillman, A. G.; Kuntz, I. D. DOCK 4.0: search strategies for automated molecular docking of flexible molecule databases. *J. Comput.-Aided Mol. Des.* **2001**, *15* (5), 411–428.

**Table 8. Pearson's Correlation Coefficients between PL-PatchSurfer Score and  $\text{pIC}_{50}$** 

protein–ligand data set	PL-PatchSurfer	Nedumpally-Govindan et al. <sup>47</sup>	Kumar et al. <sup>44</sup>	Yan et al. <sup>48</sup>	Hogues et al. <sup>45</sup>	Baumgartner et al. <sup>49</sup>	Martiny et al. <sup>46</sup>
FXa	-0.590	-0.26/-0.43	0.135	0.15/0.44/0.30/0.09	0.263/0.139	0.10/0.00/0.00/0.00	0.039
	-0.094	-0.16/-0.14		-0.11/0.08/0.14/0.19	0.088/0.057	0.35/0.30/0.44/0.36	0.077
	-0.139	-0.22/-0.16		-0.18/-0.24/-0.18/0.11	0.019/0.091	0.33/0.28/0.48/0.40	0.126
SYK	-0.244	-0.38/-0.38	0.784	0.31/0.53/0.59/0.33	0.120/0.127	0.62/0.62/0.10/0.25	0.265
TRMD	-0.671	-0.61/-0.56	0.179	0.82/0.25/0.24/0.65	0.514/0.058	0.69/0.75/0.73/0.82	0.591

Correlations of Nedumpally-Govindan et al. were taken from Figure 4 of their paper<sup>47</sup> and Kumar et al.<sup>44</sup> were taken from Table 2 of their paper. For FXa, they provided an overall correlation for the three sets. Yan et al. correlations are from Table 5 of their paper.<sup>48</sup> The first three values are IT-Score and its variations and the last one is the score by AutoDock Vina. The values for Hogues et al.<sup>45</sup> are from Table 3 of their paper. Values of Baumgartner et al.<sup>49</sup> were computed from Figure 6 of their paper. Values of Martiny et al.<sup>46</sup> were computed from  $R^2$  values in Table 3 of their paper. Since it was not clear if their score has a positive or negative correlation to  $\text{pIC}_{50}$ , we chose to put positive values.

- (4) Case, D. A.; Cheatham, T. E., 3rd; Darden, T.; Gohlke, H.; Luo, R.; Merz, K. M., Jr.; Onufriev, A.; Simmerling, C.; Wang, B.; Woods, R. J. The Amber biomolecular simulation programs. *J. Comput. Chem.* **2005**, *26* (16), 1668–1688.
- (5) Brooks, B. R.; Brooks, C. L., 3rd; Mackerell, A. D., Jr.; Nilsson, L.; Petrella, R. J.; Roux, B.; Won, Y.; Archontis, G.; Bartels, C.; Boresch, S.; Caflisch, A.; Caves, L.; Cui, Q.; Dinner, A. R.; Feig, M.; Fischer, S.; Gao, J.; Hodoscek, M.; Im, W.; Kuczera, K.; Lazaridis, T.; Ma, J.; Ovchinnikov, V.; Paci, E.; Pastor, R. W.; Post, C. B.; Pu, J. Z.; Schaefer, M.; Tidor, B.; Venable, R. M.; Woodcock, H. L.; Wu, X.; Yang, W.; York, D. M.; Karplus, M. CHARMM: the biomolecular simulation program. *J. Comput. Chem.* **2009**, *30* (10), 1545–1614.
- (6) Christen, M.; Hunenberger, P. H.; Bakowies, D.; Baron, R.; Burgi, R.; Geerke, D. P.; Heinz, T. N.; Kastenholz, M. A.; Krautler, V.; Oostenbrink, C.; Peter, C.; Trzesniak, D.; van Gunsteren, W. F. The GROMOS software for biomolecular simulation: GROMOS05. *J. Comput. Chem.* **2005**, *26* (16), 1719–1751.
- (7) Tirado-Rives, J.; Jorgensen, W. L. Viability of molecular modeling with pentium-based PCs. *J. Comput. Chem.* **1996**, *17* (11), 1385–1386.
- (8) Grinter, S. Z.; Zou, X. A Bayesian statistical approach of improving knowledge-based scoring functions for protein-ligand interactions. *J. Comput. Chem.* **2014**, *35* (12), 932–943.
- (9) Huang, S. Y.; Zou, X. An iterative knowledge-based scoring function to predict protein-ligand interactions: I. Derivation of interaction potentials. *J. Comput. Chem.* **2006**, *27* (15), 1866–1875.
- (10) Muegge, I.; Martin, Y. C. A general and fast scoring function for protein-ligand interactions: a simplified potential approach. *J. Med. Chem.* **1999**, *42* (5), 791–804.
- (11) Gohlke, H.; Hendlich, M.; Klebe, G. Knowledge-based scoring function to predict protein-ligand interactions. *J. Mol. Biol.* **2000**, *295* (2), 337–356.
- (12) Mooij, W. T.; Verdonk, M. L. General and targeted statistical potentials for protein-ligand interactions. *Proteins: Struct., Funct., Genet.* **2005**, *61* (2), 272–287.
- (13) Bohm, H. J. The development of a simple empirical scoring function to estimate the binding constant for a protein-ligand complex of known three-dimensional structure. *J. Comput.-Aided Mol. Des.* **1994**, *8* (3), 243–256.
- (14) Wang, R.; Lai, L.; Wang, S. Further development and validation of empirical scoring functions for structure-based binding affinity prediction. *J. Comput.-Aided Mol. Des.* **2002**, *16* (1), 11–26.
- (15) Korb, O.; Stutzle, T.; Exner, T. E. Empirical scoring functions for advanced protein-ligand docking with PLANTS. *J. Chem. Inf. Model.* **2009**, *49* (1), 84–96.
- (16) Eldridge, M. D.; Murray, C. W.; Auton, T. R.; Paolini, G. V.; Mee, R. P. Empirical scoring functions: I. The development of a fast empirical scoring function to estimate the binding affinity of ligands in receptor complexes. *J. Comput.-Aided Mol. Des.* **1997**, *11* (5), 425–445.
- (17) Sippl, M. J. Knowledge-based potentials for proteins. *Curr. Opin. Struct. Biol.* **1995**, *5* (2), 229–235.
- (18) Dunbar, J. B., Jr.; Smith, R. D.; Damm-Ganamet, K. L.; Ahmed, A.; Esposito, E. X.; Delproposto, J.; Chinnaswamy, K.; Kang, Y. N.; Kubish, G.; Gestwicki, J. E.; Stuckey, J. A.; Carlson, H. A. CSAR data set release 2012: ligands, affinities, complexes, and docking decoys. *J. Chem. Inf. Model.* **2013**, *53* (8), 1842–1852.
- (19) Damm-Ganamet, K. L.; Smith, R. D.; Dunbar, J. B., Jr.; Stuckey, J. A.; Carlson, H. A. CSAR benchmark exercise 2011–2012: evaluation of results from docking and relative ranking of blinded congeneric series. *J. Chem. Inf. Model.* **2013**, *53* (8), 1853–1870.
- (20) Smith, R. D.; Dunbar, J. B., Jr.; Ung, P. M.; Esposito, E. X.; Yang, C. Y.; Wang, S.; Carlson, H. A. CSAR benchmark exercise of 2010: combined evaluation across all submitted scoring functions. *J. Chem. Inf. Model.* **2011**, *51* (9), 2115–2131.
- (21) Dunbar, J. B., Jr.; Smith, R. D.; Yang, C. Y.; Ung, P. M.; Lexa, K. W.; Khazanov, N. A.; Stuckey, J. A.; Wang, S.; Carlson, H. A. CSAR benchmark exercise of 2010: selection of the protein-ligand complexes. *J. Chem. Inf. Model.* **2011**, *51* (9), 2036–2046.
- (22) Zhu, X.; Xiong, Y.; Kihara, D. Large-scale binding ligand prediction by improved patch-based method Patch-Surfer2.0. *Bioinformatics* **2015**, *31* (S), 707–713.
- (23) Sael, L.; Kihara, D. Detecting local ligand-binding site similarity in nonhomologous proteins by surface patch comparison. *Proteins: Struct., Funct., Genet.* **2012**, *80* (4), 1177–1195.
- (24) Morris, G. M.; Huey, R.; Lindstrom, W.; Sanner, M. F.; Belew, R. K.; Goodsell, D. S.; Olson, A. J. AutoDock4 and AutoDockTools4: Automated docking with selective receptor flexibility. *J. Comput. Chem.* **2009**, *30* (16), 2785–2791.
- (25) Trott, O.; Olson, A. J. AutoDock Vina: improving the speed and accuracy of docking with a new scoring function, efficient optimization, and multithreading. *J. Comput. Chem.* **2010**, *31* (2), 455–461.
- (26) Hu, B.; Zhu, X.; Monroe, L.; Bures, M. G.; Kihara, D. PL-PatchSurf: A Novel Molecular Local Surface-Based Method for Exploring Protein-Ligand Interactions. *Int. J. Mol. Sci.* **2014**, *15* (9), 15122–15145.
- (27) Shin, W. H.; Bures, M. G.; Kihara, D. PatchSurfers: Two Methods for Local Molecular Property-Based Binding Ligand Prediction. *Methods* **2015**, DOI: [10.1016/j.ymeth.2015.09.026](https://doi.org/10.1016/j.ymeth.2015.09.026).
- (28) Shin, W. H.; Zhu, X.; Bures, M. G.; Kihara, D. Three-Dimensional Compound Comparison Methods and Their Application in Drug Discovery. *Molecules* **2015**, *20* (7), 12841–12862.
- (29) Tinberg, C. E.; Khare, S. D.; Dou, J.; Doyle, L.; Nelson, J. W.; Schena, A.; Jankowski, W.; Kalodimos, C. G.; Johnsson, K.; Stoddard, B. L.; Baker, D. Computational design of ligand-binding proteins with high affinity and selectivity. *Nature* **2013**, *501* (7466), 212–216.
- (30) Canterakis, N. 3D Zernike moments and Zernike affine invariants for 3D image analysis and recognition. *Proc. 11th Scandinavian Conference on Image Analysis* **1999**, 85–93.
- (31) Sael, L.; Li, B.; La, D.; Fang, Y.; Ramani, K.; Rustamov, R.; Kihara, D. Fast protein tertiary structure retrieval based on global surface shape similarity. *Proteins: Struct., Funct., Genet.* **2008**, *72* (4), 1259–1273.
- (32) Hawkins, P. C.; Skillman, A. G.; Warren, G. L.; Ellingson, B. A.; Stahl, M. T. Conformer generation with OMEGA: algorithm and validation using high quality structures from the Protein Databank and Cambridge Structural Database. *J. Chem. Inf. Model.* **2010**, *50* (4), 572–584.
- (33) Wu, S.; Zhang, Y. LOMETS: a local meta-threading-server for protein structure prediction. *Nucleic Acids Res.* **2007**, *35* (10), 3375–3382.
- (34) Sali, A.; Blundell, T. L. Comparative protein modelling by satisfaction of spatial restraints. *J. Mol. Biol.* **1993**, *234* (3), 779–815.
- (35) Hattori, M.; Tanaka, N.; Kanehisa, M.; Goto, S. SIMCOMP/SUBCOMP: chemical structure search servers for network analyses. *Nucleic Acids Res.* **2010**, *38*, W652–W656.
- (36) Venkatraman, V.; Chakravarthy, P. R.; Kihara, D. Application of 3D Zernike descriptors to shape-based ligand similarity searching. *J. Cheminf.* **2009**, *1*, 19.
- (37) Roy, A.; Skolnick, J. LIGSIFT: an open-source tool for ligand structural alignment and virtual screening. *Bioinformatics* **2015**, *31* (4), 539–544.
- (38) O'Boyle, N. M.; Banck, M.; James, C. A.; Morley, C.; Vandermeersch, T.; Hutchison, G. R. Open Babel: An open chemical toolbox. *J. Cheminf.* **2011**, *3*, 33.
- (39) Michino, M.; Abola, E.; Brooks, C. L., 3rd; Dixon, J. S.; Moult, J.; Stevens, R. C. Community-wide assessment of GPCR structure modelling and ligand docking: GPCR Dock 2008. *Nat. Rev. Drug Discovery* **2009**, *8* (6), 455–463.
- (40) Bordogna, A.; Pandini, A.; Bonati, L. Predicting the accuracy of protein-ligand docking on homology models. *J. Comput. Chem.* **2011**, *32* (1), 81–98.
- (41) Kufareva, I.; Katritch, V.; Stevens, R. C.; Abagyan, R. Advances in GPCR modeling evaluated by the GPCR Dock 2013 assessment: meeting new challenges. *Structure* **2014**, *22* (8), 1120–1139.
- (42) Smith, R. D.; Damm-Ganamet, K. L.; Dunbar, J. B.; Ahmed, A.; Chinnaswamy, K.; Delproposto, J. E.; Kubish, G. M.; Tinberg, C. E.,

Khare, S. D.; Dou, J.; Doyle, L.; Stuckey, J. A.; Baker, D.; Carlson, H. A. CSAR Benchmark Exercise 2013: Evaluation of Results from a Combined Computational Protein Design, Docking, and Scoring/Ranking Challenge. *J. Chem. Inf. Model.* **2015**, DOI: 10.1021/acs.jcim.5b00387.

(43) Allen, W. J.; Baliaus, T. E.; Mukherjee, S.; Brozell, S. R.; Moustakas, D. T.; Lang, P. T.; Case, D. A.; Kuntz, I. D.; Rizzo, R. C. DOCK 6: Impact of new features and current docking performance. *J. Comput. Chem.* **2015**, 36 (15), 1132–1156.

(44) Kumar, A.; Zhang, K. Y. Application of Shape Similarity in Pose Selection and Virtual Screening in CSARDock2014 Exercise. *J. Chem. Inf. Model.* **2015**, DOI: 10.1021/acs.jcim.5b00279.

(45) Hogues, H.; Sulea, T.; Purisima, E. O. Evaluation of the WilmaSIE Virtual Screening Method in Community Structure-Activity Resource 2013 and 2014 Blind Challenges. *J. Chem. Inf. Model.* **2015**, DOI: 10.1021/acs.jcim.5b00278.

(46) Martiny, V. Y.; Martz, F.; Selwa, E.; Iorga, B. I. Blind Pose Prediction, Scoring, and Affinity Ranking of the CSAR 2014 Dataset. *J. Chem. Inf. Model.* **2015**, DOI: 10.1021/acs.jcim.5b00337.

(47) Nedumpully-Govindan, P.; Jemec, D. B.; Ding, F. CSAR Benchmark of Flexible MedusaDock in Affinity Prediction and Nativelike Binding Pose Selection. *J. Chem. Inf. Model.* **2015**, DOI: 10.1021/acs.jcim.5b00303.

(48) Yan, C.; Grinter, S. Z.; Merideth, B. R.; Ma, Z.; Zou, X. Iterative Knowledge-Based Scoring Functions Derived from Rigid and Flexible Decoy Structures: Evaluation with the 2013 and 2014 CSAR Benchmarks. *J. Chem. Inf. Model.* **2015**, DOI: 10.1021/acs.jcim.5b00504.

(49) Baumgartner, M. P.; Camacho, C. J. Choosing the Optimal Rigid Receptor for Docking and Scoring in the CSAR 2013/2014 Experiment. *J. Chem. Inf. Model.* **2015**, DOI: 10.1021/acs.jcim.5b00338.